

Effect of charge on negative–phase–velocity propagation of electromagnetic waves in the ergosphere of a rotating black hole

Benjamin M. Ross*, Tom G. Mackay†

School of Mathematics, University of Edinburgh, Edinburgh EH9 3JZ, UK

Akhlesh Lakhtakia‡

Department of Engineering Science and Mechanics

Pennsylvania State University, University Park, PA 16802–6812, USA

Abstract

The presence of charge promotes the propensity of a rotating black hole to support the propagation of electromagnetic plane waves with negative phase velocity (NPV) in its ergosphere, whether the Kerr–Newman or the Kerr–Sen metric descriptions of spacetime are considered. Striking differences in the NPV characteristics for the Kerr–Newman and Kerr–Sen metrics emerge from numerical studies, particularly close to the outer event horizon when the magnitude of the charge is large.

Keywords: Negative phase velocity (NPV), ergosphere, Kerr–Newman metric, Kerr–Sen metric

1 Introduction

Electromagnetic plane waves with negative phase velocity (NPV) have been the centre of much attention lately [1]. They give rise to many exotic phenomenons — the most prominent being negative refraction [2] — which are not associated with their positive phase velocity (PPV) counterparts. Much of the interest in NPV propagation has stemmed from the realization of negatively refracting metamaterials [3]. In addition, the prospects of NPV propagation in special [4] and general [5] relativistic scenarios, and the concomitant implications for observational astronomy, have prompted study and speculation within the past few years [6].

It is now well established theoretically that, for certain spacetime metrics, NPV propagation can be supported in free space [7, 8]. In particular, NPV can arise in the ergosphere of a rotating black hole described by the Kerr metric [9]. The NPV–supporting regions are concentrated towards the equator of the ergosphere, and this concentration becomes exaggerated as the angular velocity of the black hole is increased. Here we address the question: how does the presence of charge effect the propensity of a rotating black hole to support NPV propagation?

The most commonly encountered spacetime description of a charged rotating black hole is provided by the Kerr–Newman metric [10]. This solution to the Einstein field equations was derived in the 1960s [11, 12]. In 1992, Sen developed an alternative metric solution describing a charged

*Permanent address: Department of Engineering Science and Mechanics, Pennsylvania State University, University Park, PA 16802–6812, USA. email: bmr180@psu.edu

†e–mail: T.Mackay@ed.ac.uk

‡e–mail: akhlesh@psu.edu

rotating black hole, based on the action of a heterotic string [13]. Since then, various aspects of the structure and properties of this Kerr–Sen metric have been established [14, 15, 16]. In the following sections, we consider both the Kerr–Newman and the Kerr–Sen metrics in our investigation of the NPV characteristics of a charged rotating black hole.

2 Theoretical framework

2.1 Preliminaries

Electromagnetic propagation is considered in free space. The spacetime curvature is described by the metric $g_{\alpha\beta}$ [§] with signature $(+, -, -, -)$. Here we outline the theory of gravitationally assisted NPV propagation, comprehensive details being available elsewhere [5, 9].

Following the approach originally put forth by Tamm [17, 18, 19, 20], we exploit the fact that electromagnetic propagation in curved spacetime in free space is equivalent to propagation in a fictitious, instantaneously responding, bianisotropic medium in flat spacetime, characterized by the constitutive relations

$$\left. \begin{aligned} D_\ell &= \gamma_{\ell m} E_m + \varepsilon_{\ell mn} \Gamma_m H_n \\ B_\ell &= \gamma_{\ell m} H_m - \varepsilon_{\ell mn} \Gamma_m E_n \end{aligned} \right\}. \quad (1)$$

Herein, E_ℓ , B_ℓ , D_ℓ , and H_ℓ are the components of the conventional electromagnetic field vectors; $\varepsilon_{\ell mn}$ is the three-dimensional Levi-Civita symbol; and the components of the tensor $\gamma_{\ell m}$ and the vector Γ_m are defined as

$$\left. \begin{aligned} \gamma_{\ell m} &= -(-g)^{1/2} \frac{g^{\ell m}}{g_{00}} \\ \Gamma_m &= \frac{g_{0m}}{g_{00}} \end{aligned} \right\}. \quad (2)$$

In order to consider planewave propagation, we rewrite (1) in 3×3 dyadic/3 vector form as

$$\left. \begin{aligned} \underline{D}(ct, \underline{r}) &= \epsilon_0 \underline{\underline{\gamma}}(ct, \underline{r}) \cdot \underline{E}(ct, \underline{r}) - \frac{1}{c} \underline{\underline{\Gamma}}(ct, \underline{r}) \times \underline{H}(ct, \underline{r}) \\ \underline{B}(ct, \underline{r}) &= \mu_0 \underline{\underline{\gamma}}(ct, \underline{r}) \cdot \underline{H}(ct, \underline{r}) + \frac{1}{c} \underline{\underline{\Gamma}}(ct, \underline{r}) \times \underline{E}(ct, \underline{r}) \end{aligned} \right\}, \quad (3)$$

wherein $\underline{\underline{\gamma}}(ct, \underline{r})$ is the dyadic-equivalent of $\gamma_{\ell m}$, $\underline{\underline{\Gamma}}(ct, \underline{r})$ is the vector-equivalent of Γ_m , the scalar constants ϵ_0 and μ_0 denote the permittivity and permeability of vacuum in the absence of a gravitational field, and SI units are adopted. In source-free regions, \underline{E} , \underline{B} , \underline{D} , and \underline{H} are related by the Maxwell curl postulates as

$$\left. \begin{aligned} \nabla \times \underline{E}(ct, \underline{r}) + \frac{\partial}{\partial t} \underline{B}(ct, \underline{r}) &= \underline{0} \\ \nabla \times \underline{H}(ct, \underline{r}) - \frac{\partial}{\partial t} \underline{D}(ct, \underline{r}) &= \underline{0} \end{aligned} \right\}. \quad (4)$$

Let us emphasize that, while the spatial (\underline{r}) and temporal (t) coordinates have been separated in (3) and (4), the underlying spacetime remains curved.

Our aim is to explore electromagnetic planewave propagation in the spacetime of a black hole of geometric mass m_{bh} and charge q_{bh} , rotating with angular momentum a_{bh} about the Cartesian z

[§]Greek indexes take the values 0, 1, 2 and 3, Roman indexes take the values 1, 2 and 3, $x^0 = ct$, where c is the speed of light in vacuum in the absence of all gravitational fields, and $x^{1,2,3}$ represent the three spatial coordinates.

axis, in conventional units. Two different descriptions of this spacetime are considered, as provided by the Kerr–Newman metric and the Kerr–Sen metric. The line elements for these are conventionally expressed in terms of Boyer–Lindquist coordinates. In order to establish the corresponding forms of the dyadic $\underline{\underline{\gamma}}$ and vector $\underline{\Gamma}$, the Kerr–Schild Cartesian coordinate representations for these metrics are presented in the following two subsections.

2.2 Kerr–Newman spacetime

The Kerr–Newman line element is given in Boyer–Lindquist coordinates as [21, 22]

$$ds^2 = \frac{\Delta_{KN}}{R^2 + a_{\text{bh}}^2 \cos^2 \theta} (dt - a_{\text{bh}} \sin^2 \theta d\phi)^2 - \frac{\sin^2 \theta}{R^2 + a_{\text{bh}}^2 \cos^2 \theta} [(R^2 + a_{\text{bh}}^2) d\phi - a_{\text{bh}} dt]^2 - \frac{R^2 + a_{\text{bh}}^2 \cos^2 \theta}{\Delta_{KN}} dR^2 - (R^2 + a_{\text{bh}}^2 \cos^2 \theta) d\theta^2, \quad (5)$$

where R is given implicitly via

$$R^2 = x^2 + y^2 + z^2 - a_{\text{bh}}^2 \left[1 - \left(\frac{z}{R} \right)^2 \right], \quad (6)$$

and

$$\Delta_{KN} = R^2 - 2m_{\text{bh}}R + a_{\text{bh}}^2 + q_{\text{bh}}^2. \quad (7)$$

By applying the coordinate transformation $(t, \phi, R, \theta) \rightarrow (\bar{t}, x, y, z)$ specified by

$$x = (R \cos \bar{\phi} + a_{\text{bh}} \sin \bar{\phi}) \sin \theta, \quad (8)$$

$$y = (R \sin \bar{\phi} - a_{\text{bh}} \cos \bar{\phi}) \sin \theta, \quad (9)$$

$$z = R \cos \theta, \quad (10)$$

$$d\bar{t} = dt + dR - \frac{R^2 + a_{\text{bh}}^2}{\Delta_{KN}} dR, \quad (11)$$

$$d\bar{\phi} = d\phi - \frac{a_{\text{bh}}}{\Delta_{KN}} dR, \quad (12)$$

the line element (5) is expressed in Kerr–Schild Cartesian form as

$$ds^2 = d\bar{t}^2 - dx^2 - dy^2 - dz^2 - \frac{(2m_{\text{bh}}R - q_{\text{bh}}^2) R^2}{R^4 + a_{\text{bh}}^2 z^2} \times \left[d\bar{t} - \frac{z}{R} dz - \frac{R}{R^2 + a_{\text{bh}}^2} (x dx + y dy) - \frac{a_{\text{bh}}}{R^2 + a_{\text{bh}}^2} (x dy - y dx) \right]^2. \quad (13)$$

The corresponding metric components $g_{\alpha\beta}$ — from which the associated dyadic $\underline{\underline{\gamma}}$ and vector $\underline{\Gamma}$ are immediately delivered by the definitions (2) — are provided explicitly in Appendix 1.

We focus on the regime $m_{\text{bh}}^2 > a_{\text{bh}}^2$. Furthermore, our interest lies in the ergosphere demarcated as $R_+ < R < R_{S+}$, with $R = R_+$ representing the outer event horizon and $R = R_{S+}$ representing the stationary limit surface [23]. The outer event horizon occurs where $\Delta_{KN} = 0$. Thus,

$$R_+ = m_{\text{bh}} + \sqrt{m_{\text{bh}}^2 - a_{\text{bh}}^2 - q_{\text{bh}}^2}. \quad (14)$$

The stationary limit surface $R = R_{S+}$ occurs where $g_{00} = 0$. Thus,

$$R_{S+} = m_{\text{bh}} + \sqrt{m_{\text{bh}}^2 - q_{\text{bh}}^2 - \left(\frac{a_{\text{bh}} z}{R_{S+}} \right)^2}. \quad (15)$$

2.3 Kerr–Sen spacetime

We now turn to the Kerr–Sen line element which is given in Boyer–Lindquist coordinates as [14, 16]

$$ds^2 = \frac{\Delta_{KS}}{\tilde{S}^2 + a_{\text{bh}}^2 \cos^2 \theta} (dt - a_{\text{bh}} \sin^2 \theta d\phi)^2 - \frac{\sin^2 \theta}{\tilde{S}^2 + a_{\text{bh}}^2 \cos^2 \theta} \left[(\tilde{S}^2 + a_{\text{bh}}^2) d\phi - a_{\text{bh}} dt \right]^2 - \frac{\tilde{S}^2 + a_{\text{bh}}^2 \cos^2 \theta}{\Delta_{KS}} dS^2 - (\tilde{S}^2 + a_{\text{bh}}^2 \cos^2 \theta) d\theta^2, \quad (16)$$

where

$$\Delta_{KS} = S^2 - 2 \left(m_{\text{bh}} - \frac{\beta}{2} \right) S + a_{\text{bh}}^2, \quad (17)$$

$$\tilde{S}^2 = S^2 + \beta S, \quad (18)$$

$$\beta = \frac{q_{\text{bh}}^2}{m_{\text{bh}}}, \quad (19)$$

and \tilde{S} satisfies

$$\tilde{S}^2 = x^2 + y^2 + z^2 - a_{\text{bh}}^2 \left[1 - \left(\frac{z}{\tilde{S}} \right)^2 \right]. \quad (20)$$

Under the coordinate transformation $(t, \phi, S, \theta) \rightarrow (\bar{t}, x, y, z)$ specified by

$$x = (\tilde{S} \cos \bar{\phi} + a_{\text{bh}} \sin \bar{\phi}) \sin \theta, \quad (21)$$

$$y = (\tilde{S} \sin \bar{\phi} - a_{\text{bh}} \cos \bar{\phi}) \sin \theta, \quad (22)$$

$$z = \tilde{S} \cos \theta, \quad (23)$$

$$d\bar{t} = dt + d\tilde{S} - \frac{\tilde{S}^2 + a_{\text{bh}}^2}{\Delta_{KS}} d\tilde{S}, \quad (24)$$

$$d\bar{\phi} = d\phi - \frac{a_{\text{bh}}}{\Delta_{KS}} d\tilde{S}, \quad (25)$$

the Kerr–Schild Cartesian form of the line element (16) emerges as

$$ds^2 = d\bar{t}^2 - dx^2 - dy^2 - dz^2 + \frac{\beta^2 (\tilde{S}^2 + a_{\text{bh}}^2 \cos^2 \theta)}{(\beta^2 + 4\tilde{S}^2) \Delta_{KS}} d\tilde{S}^2 - \frac{2m_{\text{bh}} \tilde{S}^2 S}{\tilde{S}^4 + a_{\text{bh}}^2 z^2} \times \left[d\bar{t} - \frac{z}{\tilde{S}} dz - \frac{\tilde{S}}{\tilde{S}^2 + a_{\text{bh}}^2} (x dx + y dy) - \frac{a_{\text{bh}}}{\tilde{S}^2 + a_{\text{bh}}^2} (x dy - y dx) \right]^2. \quad (26)$$

In Appendix 2, explicit expressions for the corresponding metric components $g_{\alpha\beta}$ are presented. From these, the associated dyadic $\underline{\underline{\gamma}}$ and vector $\underline{\Gamma}$ immediately delivered by the definitions (2).

In analogous manner to the case for the Kerr–Newman metric, the outer event horizon arises at $S = S_+$ with

$$S_+ = m_{\text{bh}} - \frac{\beta}{2} + \sqrt{\left(m_{\text{bh}} - \frac{\beta}{2} \right)^2 - a_{\text{bh}}^2}, \quad (27)$$

whereas the stationary limit surface arises at $S = S_{S_+}$ with

$$S_{S_+} = m_{\text{bh}} - \frac{\beta}{2} + \sqrt{\left(m_{\text{bh}} - \frac{\beta}{2}\right)^2 - \left(\frac{a_{\text{bh}} z}{\tilde{S}_{S_+}}\right)^2}. \quad (28)$$

As in §2.2, the ergosphere is the region bounded by the outer event horizon and the stationary limit surface; i.e., $S_+ < S < S_{S_+}$.

2.4 Planewave propagation

Now we turn to the propagation of plane waves in the medium characterized by (3). By choosing a sufficiently small neighbourhood \mathcal{R} specified by the Cartesian coordinates $(\tilde{x}, \tilde{y}, \tilde{z})$, we approximate the non-uniform metric $g_{\alpha\beta}$ with the uniform metric $\tilde{g}_{\alpha\beta}$ throughout \mathcal{R} [7]. Within the neighbourhood \mathcal{R} , we utilize the uniform 3×3 dyadic $\underline{\tilde{\gamma}} \equiv \underline{\underline{\gamma}}|_{\mathcal{R}}$ and the uniform 3 vector $\underline{\tilde{\Gamma}} \equiv \underline{\underline{\Gamma}}|_{\mathcal{R}}$, where $\underline{\tilde{\gamma}}$ and $\underline{\tilde{\Gamma}}$ are calculated from (2). Due to the uniform approximation, attention is restricted to electromagnetic wavelengths that are small compared to the linear dimensions of \mathcal{R} .

The three-dimensional Fourier transforms

$$\left. \begin{aligned} \underline{E}(ct, \underline{r}) &= \frac{1}{c} \int_{-\infty}^{\infty} \int_{-\infty}^{\infty} \int_{-\infty}^{\infty} \underline{E}(\omega/c, \underline{k}) \exp[i(\underline{k} \cdot \underline{r} - \omega t)] d\omega dk_1 dk_2 \\ \underline{H}(ct, \underline{r}) &= \frac{1}{c} \int_{-\infty}^{\infty} \int_{-\infty}^{\infty} \int_{-\infty}^{\infty} \underline{H}(\omega/c, \underline{k}) \exp[i(\underline{k} \cdot \underline{r} - \omega t)] d\omega dk_1 dk_2 \end{aligned} \right\}, \quad (29)$$

decompose the electromagnetic fields within \mathcal{R} . Here, the wavevector \underline{k} is the Fourier variable corresponding to \underline{r} , $i = \sqrt{-1}$ and ω is the usual temporal frequency. By combining (4) and (29), and then solving the resulting 4×4 eigenvalue problem, the wavevector component k_3 is determined [24]. Only propagating (non-evanescent) plane waves are considered; i.e., $k_3 \in \mathbb{R}$.

NPV propagation occurs when the phase velocity vector casts a negative projection on to the time-averaged Poynting vector — i.e.,

$$\underline{k} \cdot \langle \underline{P}(\omega/c, \underline{k}) \rangle_t < 0, \quad (30)$$

where the time-averaged Poynting vector $\langle \underline{P}(\omega/c, \underline{k}) \rangle_t$ is calculated from the complex-valued phasors of the electric and magnetic fields, $\underline{E}(\omega/c, \underline{k})$ and $\underline{H}(\omega/c, \underline{k})$. The left side of (30) is given by [9]

$$\underline{k} \cdot \langle \underline{P}(\omega/c, \underline{k}) \rangle_t = \frac{1}{2\omega\mu_0|\underline{\tilde{\gamma}}|} \left(|A_a|^2 \underline{e}_a \cdot \underline{\tilde{\gamma}} \cdot \underline{e}_a + |A_b|^2 \underline{e}_b \cdot \underline{\tilde{\gamma}} \cdot \underline{e}_b \right) \underline{k} \cdot \underline{\tilde{\gamma}} \cdot \underline{p}. \quad (31)$$

The complex-valued amplitudes $A_{a,b}(\omega/c, \underline{k})$ are fixed by initial and boundary conditions, whereas the unit vectors

$$\left. \begin{aligned} \underline{e}_a &= \frac{\underline{\tilde{\gamma}}^{-1} \cdot \underline{w}}{|\underline{\tilde{\gamma}}^{-1} \cdot \underline{w}|} \\ \underline{e}_b &= \frac{\underline{\tilde{\gamma}}^{-1} \cdot (\underline{p} \times \underline{e}_a)}{|\underline{\tilde{\gamma}}^{-1} \cdot (\underline{p} \times \underline{e}_a)|} \end{aligned} \right\}. \quad (32)$$

For the numerical results presented in the following section, we have chosen

$$\underline{w} = \begin{cases} \frac{1}{\sqrt{2p_z^2 + (p_x + p_y)^2}} (p_z, p_z, -p_x - p_y) & \text{for } p_z \neq 0 \\ \frac{1}{\sqrt{p_y^2 + p_x^2}} (p_y, -p_x, 0) & \text{for } p_z = 0 \end{cases}, \quad (33)$$

with $\underline{p} \equiv (p_x, p_y, p_z)$ in the Cartesian coordinate system.

For both the Kerr–Newman and Kerr–Sen metrics $|\underline{\tilde{\gamma}}| > 0$. Hence, the sufficient condition for NPV propagation

$$\left. \begin{array}{l} P_a < 0 \\ P_b < 0 \end{array} \right\} \quad (34)$$

arises, wherein

$$\left. \begin{array}{l} P_a = \left(\underline{\mathbf{e}}_a \cdot \underline{\tilde{\gamma}} \cdot \underline{\mathbf{e}}_a \right) \left(\underline{\mathbf{k}} \cdot \underline{\tilde{\gamma}} \cdot \underline{\mathbf{p}} \right) \\ P_b = \left(\underline{\mathbf{e}}_b \cdot \underline{\tilde{\gamma}} \cdot \underline{\mathbf{e}}_b \right) \left(\underline{\mathbf{k}} \cdot \underline{\tilde{\gamma}} \cdot \underline{\mathbf{p}} \right) \end{array} \right\}. \quad (35)$$

The two wavenumbers $k = k^\pm$ given by

$$k^\pm = \frac{\omega}{c} \left(\frac{\hat{\mathbf{k}} \cdot \underline{\tilde{\gamma}} \cdot \underline{\tilde{\Gamma}} \pm \sqrt{\left(\hat{\mathbf{k}} \cdot \underline{\tilde{\gamma}} \cdot \underline{\tilde{\Gamma}} \right)^2 - \hat{\mathbf{k}} \cdot \underline{\tilde{\gamma}} \cdot \hat{\mathbf{k}} \left(\underline{\tilde{\Gamma}} \cdot \underline{\tilde{\gamma}} \cdot \underline{\tilde{\Gamma}} - |\underline{\tilde{\gamma}}| \right)}}{\hat{\mathbf{k}} \cdot \underline{\tilde{\gamma}} \cdot \hat{\mathbf{k}}} \right) \quad (36)$$

develop for the arbitrarily oriented wavevector $\underline{\mathbf{k}} = k \hat{\mathbf{k}}$ with $\hat{\mathbf{k}} = (\sin \theta \cos \phi, \sin \theta \sin \phi, \cos \theta)$.

3 Numerical results

The NPV characteristics of an uncharged rotating black hole, as described by the Kerr metric, have been established previously [9]. In this section, we report on the effect that charge has on the propensity for a rotating black hole to support NPV propagation in its ergosphere. This study was carried out by numerically evaluating (31), for both the Kerr–Newman and Kerr–Sen descriptions of the blackhole spacetime.

The following strategy was implemented: for fixed values of m_{bh} , a_{bh} and q_{bh} , we considered surfaces of constant R for the Kerr–Newman metric, and surfaces of constant S for the Kerr–Sen metric, with all surfaces being contained within the respective blackhole ergospheres. The prospects for NPV propagation for all propagation directions $\hat{\mathbf{k}} = (\sin \theta \cos \phi, \sin \theta \sin \phi, \cos \theta)$ were calculated over a grid of points on surfaces of constant R and S . At each coordinate point $(\tilde{x}, \tilde{y}, \tilde{z})$ on the grid, the quantities P_a and P_b were computed at 1° increments for $\theta \in [0^\circ, 180^\circ)$ and $\phi \in [0^\circ, 360^\circ)$, for both $k = k^+$ and $k = k^-$. For each value of (θ, ϕ) at which NPV was found to be supported (i.e., $P_a < 0$ and $P_b < 0$), a score of one point was assigned to the $(\tilde{x}, \tilde{y}, \tilde{z})$ grid point. The total score at each grid point was translated to a colour for the convenient presentation of results.

Figure 1 shows the NPV propagation maps for Kerr–Newman spacetime for a charged rotating black hole with $a_{\text{bh}} = m_{\text{bh}} \sqrt{3/4}$. Three constant R surfaces within the ergosphere are considered,

namely $R = 0.99R_+ + 0.01R_{S_+}$ (in Figures 1(a) and (d)); $R = 0.5R_+ + 0.5R_{S_+}$ (in Figures 1(b) and (e)); and $R = 0.01R_+ + 0.99R_{S_+}$ (in Figures 1(c) and (f)). For each surface, a small value of q_{bh} ($q_{\text{bh}} = 0.1$ in Figure 1(a), (b), and (c)) and a large value of q_{bh} ($q_{\text{bh}} = 0.45$ in Figure 1(d), (e), and (f)) are chosen. We note that $q_{\text{bh}} \leq 0.5$ in order for the ergosphere boundaries to remain real-valued.

In Figure 1(a)–(c) that, for $q_{\text{bh}} = 0.1$, the regions of NPV propagation are most heavily concentrated near the equator of the ergosphere and NPV becomes less likely towards the poles. Also, NPV propagation is more likely near the outer event horizon and less likely near the stationary limit surface. Increasing the value of q_{bh} does not markedly change the qualitative nature of the NPV characteristics, as illustrated by Figure 1(d)–(f). However, the incidence of NPV propagation is considerably greater at $q_{\text{bh}} = 0.45$ as compared with $q_{\text{bh}} = 0.1$, at all three constant R surfaces.

The corresponding NPV propagation maps calculated using the Kerr–Sen metric are presented in Figure 2. A comparison of Figure 2(a)–(c) with Figure 1(a)–(c) reveals that the NPV characteristics of the Kerr–Sen and Kerr–Newman metrics are quite similar at $q_{\text{bh}} = 0.1$. However, stark differences between the Kerr–Sen and Kerr–Newman NPV characteristics emerge at $q_{\text{bh}} = 0.45$, particularly near to the outer event horizon. For the Kerr–Sen metric, we see in Figure 2(d) that the distribution of NPV propagation is concentrated in a region between the ergosphere pole and equator, while a relatively low incidence occurs at the equator. This is quite different from the situation for the Kerr–Newman metric that is displayed in Figure 1(d).

We note that the NPV propagation maps at $q_{\text{bh}} = 0.1$, for both the Kerr–Newman metric and Kerr–Sen metric, are quite similar to those reported for the uncharged rotating black hole [9]. This reflects the fact that both the Kerr–Newman metric and the Kerr–Sen metric become identical to the Kerr metric in the limit $q_{\text{bh}} \rightarrow 0$. Furthermore, regardless of charge, NPV is not supported at the ergosphere pole.

4 Concluding remarks

Our investigation has revealed that the propensity for a rotating black hole to support NPV propagation is highly sensitive to the presence of charge in the black hole. Specifically,

- the overall incidence of NPV increases as q_{bh} increases, for both the Kerr–Newman and Kerr–Sen metrics;
- as q_{bh} increases, differences in the NPV characteristics associated with the Kerr–Newman and Kerr–Sen metrics emerge; and
- the greatest differences between the NPV characteristics of the Kerr–Newman and the Kerr–Sen metrics arise close to the outer event horizons of their respective ergospheres.

These findings suggest the possibility of a NPV–based experiment to distinguish between the Kerr–Newman and Kerr–Sen metric descriptions of a charged rotating black hole.

Acknowledgements: BMR is supported by a UK EPSRC (grant GR/S60631/01) and a US NSF Graduate Research Fellowship. TGM and AL thank Dr. Sandi Setiawan (University of Edinburgh)

for suggesting this study and Prof. Malcolm MacCallum (Queen Mary, University of London) for his assistance with §2.3.

References

- [1] Lakhtakia A, McCall MW, and Weiglhofer WS 2003 Negative phase-velocity mediums *Introduction to Complex Mediums for Optics and Electromagnetics* ed WS Weiglhofer and A Lakhtakia (Bellingham, WA, USA: SPIE Press) pp347–363
- [2] Ramakrishna SA 2005 Physics of negative refractive index materials *Rep. Prog. Phys.* **68** 449–521
- [3] Shelby RA, Smith DR and Schultz S 2001 Experimental verification of a negative index of refraction *Science* **292** 77–79
- [4] Mackay TG and Lakhtakia A 2004 Negative phase velocity in a uniformly moving, homogeneous, isotropic, dielectric-magnetic medium *J. Phys. A: Math. Gen.* **37** 5697–5711
- [5] Mackay TG, Lakhtakia A and Setiawan S 2005 Gravitation and electromagnetic wave propagation with negative phase velocity *New J. Phys.* **7** 75
- [6] Mackay TG and Lakhtakia A 2006 Gravity-induced negative refraction of electromagnetic waves *Current Sci.* **90** 640–641
- [7] Lakhtakia A, Mackay TG and Setiawan S 2005 Global and local perspectives of gravitationally assisted negative-phase-velocity propagation of electromagnetic waves in vacuum *Phys. Lett. A* **336** 89–96
- [8] Mackay TG, Lakhtakia A and Setiawan S 2005 Electromagnetic waves with negative phase velocity in Schwarzschild-de Sitter spacetime *Europhys. Lett.* **71** 925–931
- [9] Mackay TG, Lakhtakia A and Setiawan S 2005 Electromagnetic negative-phase-velocity propagation in the ergosphere of a rotating black hole *New J. Phys.* **7** 171
- [10] Stephani H, Kramer D, MacCallum MAH, Hoenselaers C and Herlt E 2003 *Exact Solutions of Einstein's Field Equations, 2nd ed* (Cambridge: Cambridge University Press) Chap 32
- [11] Kerr RP 1963 Gravitational field of a spinning mass as an example of algebraically special metrics *Phys. Rev. Lett.* **11** 237–238
- [12] Newman ET, Couch E, Chinnapared K, Exton A, Prakash A and Torrence R 1965 Metric of a rotating charged mass *J. Math. Phys.* **6** 918–919
- [13] Sen A 1992 Rotating charged black hole solution in heterotic string theory *Phys. Rev. Lett.* **69** 1006–1009
- [14] Okai T 1994 Global structure and thermodynamic property of the 4-dimensional twisted Kerr solution *Prog. Theor. Phys.* **92** 47–65
- [15] Blaga PA and Blaga C 2001 Bounded radial geodesics around a Kerr-Sen black hole *Class. Quantum Grav.* **18** 3893–3905

- [16] Wu SQ and Cai X 2003 Massive complex scalar field in the Kerr-Sen geometry: Exact solution of wave equation and Hawking radiation *J. Math. Phys.* **44** 1084–1088
- [17] Skrotskii GV 1957 The influence of gravitation on the propagation of light *Soviet Phys.–Dokl.* **2** 226–229
- [18] Plebanski J 1960 Electromagnetic waves in gravitational fields *Phys. Rev.* **118** 1396–1408
- [19] Landau LD and Lifshitz EM 1975 *The Classical Theory of Fields* (Oxford, UK: Clarendon Press) §90
- [20] Schleich W and Scully MO 1984 General relativity and modern optics *New Trends in Atomic Physics* ed G Grynberg and R Stora (Amsterdam, Holland: Elsevier Science Publishers) pp995–1124
- [21] Bose S and Naing TZ 1999 Quasilocal energy for rotating charged black hole solutions in general relativity and string theory *Phys. Rev. D* **60** 104027
- [22] Xulu SS 2000 Møller energy for the Kerr–Newman metric *Mod. Phys. Lett. A* **15** 1511–1517
- [23] d’Inverno R 1992 *Introducing Einstein’s Relativity* (Oxford, UK: Clarendon Press) Chap 19
- [24] Lakhtakia A 1992 General schema for the Brewster conditions *Optik* **90** 184–186

Appendix 1

The components of the Kerr–Newman metric obtained from the line element (13) expressed in Kerr–Schild Cartesian form are

$$g_{00} = 1 - \delta_{KN}, \quad (37)$$

$$g_{01} = \sigma((-1 + \delta_{KN})R^3x\tau^2 + \Delta_{KN}\{-a_{bh}\delta_{KN}[R^3(a_{bh}x + Ry) + a_{bh}(-Rx + a_{bh}y)z^2] + R^3x\tau\}), \quad (38)$$

$$g_{02} = \sigma((-1 + \delta_{KN})R^3y\tau^2 + \Delta_{KN}\{a_{bh}\delta_{KN}[R^3(Rx - a_{bh}y) + a_{bh}z^2(a_{bh}x + Ry)] + R^3y\tau\}), \quad (39)$$

$$g_{03} = \frac{z\sigma\tau}{R}\{\Delta_{KN}R^4 + a_{bh}^2\Delta_{KN}[-(-1 + \delta_{KN})R^2 + \delta_{KN}z^2] + (-1 + \delta_{KN})R^2\tau^2\}, \quad (40)$$

$$\begin{aligned} g_{11} = & -\sigma^2((-1 + \delta_{KN})R^6x^2\tau^4 - 2\Delta_{KN}R^3x\tau^2\{a_{bh}\delta_{KN}[R^3(a_{bh}x + Ry) + a_{bh}z^2(-Rx + a_{bh}y)] \\ & - R^3x\tau\} + \Delta_{KN}^2\{a_{bh}^2\delta_{KN}[R^3(a_{bh}x + Ry) + a_{bh}z^2(-Rx + a_{bh}y)]^2 \\ & + (R^8 - R^6x^2 + 2a_{bh}^2R^4z^2 + a_{bh}^4z^4)\tau^2\}), \end{aligned} \quad (41)$$

$$\begin{aligned} g_{12} = & \sigma^2\left(\frac{R^6xy(\Delta_{KN} - \tau)^2}{\tau^2} + \delta_{KN}\{a_{bh}\Delta_{KN}[R^3(a_{bh}x + Ry) + a_{bh}(-Rx + a_{bh}y)z^2] \right. \\ & \left. - R^3x\tau^2\}\{a_{bh}\Delta_{KN}[R^3(Rx - a_{bh}y) + a_{bh}(a_{bh}x + Ry)z^2] + R^3y\tau^2\}\right), \end{aligned} \quad (42)$$

$$g_{13} = \frac{z\sigma^2\tau}{R}(R^5x(\Delta_{KN} - \tau)^2\tau^2 - \delta_{KN}[a_{\text{bh}}^2\Delta_{KN}(-R^2 + z^2) + R^2\tau^2]\{-a_{\text{bh}}\Delta_{KN}[R^3(a_{\text{bh}}x + Ry) + a_{\text{bh}}(-Rx + a_{\text{bh}}y)z^2] + R^3x\tau^2\}), \quad (43)$$

$$g_{22} = -\sigma^2(a_{\text{bh}}^2\delta_{KN}\Delta_{KN}^2[R^3(Rx - a_{\text{bh}}y) + a_{\text{bh}}(a_{\text{bh}}x + Ry)z^2]^2 + \Delta_{KN}\{R^6[\Delta_{KN}(R - y)(R + y) + 2a_{\text{bh}}\delta_{KN}y(Rx - a_{\text{bh}}y)] + 2a_{\text{bh}}^2R^3[\Delta_{KN}R + \delta_{KN}y(a_{\text{bh}}x + Ry)]z^2\}a_{\text{bh}}^4\Delta_{KN}z^4)\tau^2 + 2\Delta_{KN}R^6y^2\tau^3 + (-1 + \delta_{KN})R^6y^2\tau^4, \quad (44)$$

$$g_{23} = \frac{z\sigma^2\tau}{R}(R^5y(\Delta_{KN} - \tau)^2\tau^2 - \delta_{KN}[a_{\text{bh}}^2\Delta_{KN}(-R^2 + z^2) + R^2\tau^2] \times \{a_{\text{bh}}\Delta_{KN}[R^3(Rx - a_{\text{bh}}y) + a_{\text{bh}}(a_{\text{bh}}x + Ry)z^2] + R^3y\tau^2\}), \quad (45)$$

$$g_{33} = \frac{-1}{R^2}(\sigma^2\tau^2\{\Delta_{KN}^2(R - z)(R + z)[R^8 + a_{\text{bh}}^4(-1 + \delta_{KN})R^2z^2 - a_{\text{bh}}^4\delta_{KN}z^4] + 2\Delta_{KN}R^2z^2[R^4 + a_{\text{bh}}^2(R^2 - \delta_{KN}R^2 + \delta_{KN}z^2)]\tau^2 + (-1 + \delta_{KN})R^4z^2\tau^4\}), \quad (46)$$

and $g_{\alpha\beta} = g_{\beta\alpha}$. Also,

$$\delta_{KN} = \frac{R^2(2m_{\text{bh}}R - q^2)}{R^4 + a_{\text{bh}}^2z^2}, \quad (47)$$

$$\tau = a_{\text{bh}}^2 + R^2, \quad (48)$$

$$\sigma = \frac{1}{\Delta_{KN}\tau(R^4 + a_{\text{bh}}^2z^2)}. \quad (49)$$

Appendix 2

The components of the Kerr–Sen metric obtained from the line element (26) expressed in Kerr–Schild Cartesian form are

$$g_{00} = 1 - \delta_{KS}, \quad (50)$$

$$g_{01} = \Phi\{(-1 + \delta_{KS})S^3x[-2a_{\text{bh}}^2\Delta_{KS}S + \nu(-\Delta_{KS}\beta + \rho\nu)] + 2\Delta_{KS}\tilde{S}[-a_{\text{bh}}\delta_{KS}y(S^4 + a_{\text{bh}}^2z^2) + x(S^4 + a_{\text{bh}}^2\delta_{KS}z^2)\tilde{S}]\}, \quad (51)$$

$$g_{02} = \Phi\{(-1 + \delta_{KS})S^3y[-2a_{\text{bh}}^2\Delta_{KS}S + \nu(-\Delta_{KS}\beta + \rho\nu)] + 2\Delta_{KS}\tilde{S}[a_{\text{bh}}\delta_{KS}x(S^4 + a_{\text{bh}}^2z^2) + y(S^4 + a_{\text{bh}}^2\delta_{KS}z^2)\tilde{S}]\}, \quad (52)$$

$$g_{03} = \nu\Phi[\Delta_{KS}z\{2\{S^4 + a_{\text{bh}}^2[-(-1 + \delta_{KS})S^2 + \delta_{KS}z^2]\} - (-1 + \delta_{KS})S(a_{\text{bh}}^2 + S^2)\beta\} + (-1 + \delta_{KS})S(a_{\text{bh}}^2 + S^2)z\rho\nu], \quad (53)$$

$$\begin{aligned}
g_{11} = & \Phi^2 \{ S^6 x^2 [-(-1 + \delta_{KS}) \{ 2a_{\text{bh}}^2 \Delta_{KS} S + \nu [\Delta_{KS} \beta - \rho \nu] \}^2 + \Delta_{KS}^2 (2a_{\text{bh}}^2 S + \beta \nu)^2 \zeta] \\
& + 4 \Delta_{KS} \tilde{S} [a_{\text{bh}} \delta_{KS} S^3 xy (S^4 + a_{\text{bh}}^2 z^2) [-2a_{\text{bh}}^2 \Delta_{KS} S + \nu (-\Delta_{KS} \beta + 2S\nu + \beta \nu)] \\
& - [a_{\text{bh}}^8 \Delta_{KS} z^4 + a_{\text{bh}}^6 \Delta_{KS} z^2 (2S^4 + \delta_{KS} y^2 z^2) + a_{\text{bh}}^4 \Delta_{KS} S^4 [S^4 + 2\delta_{KS} (-x^2 + y^2) z^2] \\
& + S^7 x^2 \nu [\rho \nu - \Delta_{KS} \beta (1 + \zeta)] + a_{\text{bh}}^2 S^3 (\delta_{KS} x^2 z^2 \rho \nu^2 - \Delta_{KS} \{ \delta_{KS} x^2 z^2 \beta \nu \\
& + S^5 [-\delta_{KS} y^2 + 2x^2 (1 + \zeta)] \}] \tilde{S} + 2a_{\text{bh}}^3 \delta_{KS} \Delta_{KS} xy z^2 (S^4 + a_{\text{bh}}^2 z^2) \tilde{S}^2 - \Delta_{KS} [2a_{\text{bh}}^2 S^8 \\
& + 2a_{\text{bh}}^6 z^4 + a_{\text{bh}}^4 (4S^4 z^2 + \delta_{KS} x^2 z^4) - S^8 x^2 (1 + \zeta)] \tilde{S}^3 - \Delta_{KS} (S^4 + a_{\text{bh}}^2 z^2)^2 \tilde{S}^5 \}], \quad (54)
\end{aligned}$$

$$\begin{aligned}
g_{12} = & \Delta_{KS}^2 \nu^2 \Phi^2 \left[\frac{S^6 xy \rho^2 (\Delta_{KS} - \nu)^2}{\Delta_{KS}^2} + S^6 xy \rho^2 \zeta + \frac{1}{\Delta_{KS}^2 \nu^2} (\delta_{KS} (S^3 x \{ 2a_{\text{bh}}^2 \Delta_{KS} S \right. \\
& + \nu [\Delta_{KS} \beta - \rho \nu] \} + 2a_{\text{bh}} \Delta_{KS} \tilde{S} (y (S^4 + a_{\text{bh}}^2 z^2) - a_{\text{bh}} x z^2 \tilde{S})) \{ S^3 y \{ -2a_{\text{bh}}^2 \Delta_{KS} S \\
& + \nu [-\Delta_{KS} \beta + \rho \nu] \} + 2a_{\text{bh}} \Delta_{KS} \tilde{S} [x (S^4 + a_{\text{bh}}^2 z^2) + a_{\text{bh}} y z^2 \tilde{S}] \} \}], \quad (55)
\end{aligned}$$

$$\begin{aligned}
g_{13} = & \Delta_{KS}^2 z \nu^2 \Phi^2 \left\{ \frac{S^4 (a_{\text{bh}}^2 + S^2) x \rho^2 (\Delta_{KS} - \nu)^2}{\Delta_{KS}^2} + S^4 (a_{\text{bh}}^2 + S^2) x \rho^2 \zeta \right. \\
& - \frac{1}{\Delta_{KS}^2 \nu} [\delta_{KS} \{ \Delta_{KS} S^3 \beta + a_{\text{bh}}^2 \Delta_{KS} [-2z^2 + S\rho] - S (a_{\text{bh}}^2 + S^2) \rho \nu \} (S^3 x \{ 2a_{\text{bh}}^2 \Delta_{KS} S \\
& + \nu [\Delta_{KS} \beta - \rho \nu] \} + 2a_{\text{bh}} \Delta_{KS} \tilde{S} [y (S^4 + a_{\text{bh}}^2 z^2) - a_{\text{bh}} x z^2 \tilde{S}] \} \}], \quad (56)
\end{aligned}$$

$$\begin{aligned}
g_{22} = & -\Phi^2 \{ S^6 y^2 \{ -\Delta_{KS}^2 (2a_{\text{bh}}^2 S + \beta \nu)^2 \zeta + (-1 + \delta_{KS}) [2a_{\text{bh}}^2 \Delta_{KS} S + \nu (\Delta_{KS} \beta - \nu \rho)]^2 \} \\
& + 4 \Delta_{KS} \tilde{S} [a_{\text{bh}} \delta_{KS} S^3 xy (S^4 + a_{\text{bh}}^2 z^2) [-2a_{\text{bh}}^2 \Delta_{KS} S + \nu (-\Delta_{KS} \beta + \nu \rho)] + \tilde{S} (a_{\text{bh}}^8 \Delta_{KS} z^4 \\
& + a_{\text{bh}}^6 \Delta_{KS} z^2 (2S^4 + \delta_{KS} x^2 z^2) + a_{\text{bh}}^4 \Delta_{KS} S^4 [S^4 + 2\delta_{KS} (x - y) (x + y) z^2] \\
& + S^7 y^2 \nu [-\Delta_{KS} \beta (1 + \zeta) + \nu \rho] + a_{\text{bh}}^2 S^3 [-2\Delta_{KS} S^5 y^2 (1 + \zeta) + \delta_{KS} (\Delta_{KS} S^5 x^2 \\
& - \Delta_{KS} y^2 z^2 \beta \nu + y^2 z^2 \nu^2 \rho)] + \Delta_{KS} \tilde{S} \{ 2a_{\text{bh}}^3 \delta_{KS} xy z^2 (S^4 + a_{\text{bh}}^2 z^2) + [2a_{\text{bh}}^2 S^8 + 2a_{\text{bh}}^6 z^4 \\
& + a_{\text{bh}}^4 (4S^4 z^2 + \delta_{KS} y^2 z^4) - S^8 y^2 (1 + \zeta)] \tilde{S} + (S^4 + a_{\text{bh}}^2 z^2)^2 \tilde{S}^3 \} \}], \quad (57)
\end{aligned}$$

$$\begin{aligned}
g_{23} = & \Delta_{KS}^2 z \nu^2 \Phi^2 \left[\frac{S^4 (a_{\text{bh}}^2 + S^2) y (\Delta_{KS} - \nu)^2 \rho^2}{\Delta_{KS}^2} + S^4 (a_{\text{bh}}^2 + S^2) y \zeta \rho^2 \right. \\
& + \frac{1}{\Delta_{KS}^2 \nu} (\delta_{KS} \{ a_{\text{bh}}^2 [-2\Delta_{KS} z^2 + S (\Delta_{KS} - \nu) \rho] \\
& + S^3 (\Delta_{KS} \beta - \nu \rho) \} \{ S^3 y (-2a_{\text{bh}}^2 \Delta_{KS} S + \nu (-\Delta_{KS} \beta + \nu \rho)) \\
& + 2a_{\text{bh}} \Delta_{KS} \tilde{S} [x (S^4 + a_{\text{bh}}^2 z^2) + a_{\text{bh}} y z^2 \tilde{S}] \} \}], \quad (58)
\end{aligned}$$

$$\begin{aligned}
g_{33} = & \nu^2 \Phi^2 \{ z^2 (\Delta_{KS}^2 S^6 [4S^2(1+\zeta) + 4S\beta(1+\zeta) + \beta^2(1+\zeta - \delta_{KS})] \\
& - 2a_{\text{bh}}^6 S [2(-1 + \delta_{KS})S^2(-\Delta_{KS} + S^2) + 2\delta_{KS}\Delta_{KS}z^2 \\
& + (-1 + \delta_{KS})S(-\Delta_{KS} + S^2)\beta] \rho - a_{\text{bh}}^8 (-1 + \delta_{KS})S^2 \rho^2 + 2a_{\text{bh}}^2 \Delta_{KS} S^3 \{ \Delta_{KS} [2\delta_{KS}z^2 \beta \\
& - 2S^2 \beta(-2 + \delta_{KS} - 2\zeta) + 4S^3(1+\zeta) + S\beta^2(1 - \delta_{KS} + \zeta)] + S^3(\delta_{KS}\beta - \rho)\rho \} \\
& + a_{\text{bh}}^4 \{ \Delta_{KS}^2 (-4\delta_{KS}z^4 + 4\delta_{KS}S z^2 \beta + 4S^3 \beta(1 - \delta_{KS} + \zeta) \\
& + S^4(4 - 4\delta_{KS} + 4\zeta) + S^2(8\delta_{KS}z^2 + \beta^2 - \delta_{KS}\beta^2 + \beta^2\zeta) \} + 4\Delta_{KS} S^3 [(-2 + \delta_{KS})S^2 \\
& - \delta_{KS}z^2 + (-1 + \delta_{KS})S\beta] \rho - (-1 + \delta_{KS})S^6 \rho^2 \} - 2[2\Delta_{KS}^2 (S^4 + a_{\text{bh}}^2 z^2)^2 \\
& + \Delta_{KS} S (a_{\text{bh}}^2 + S^2) z^2 (2\{S^4 + a_{\text{bh}}^2 [-(-1 + \delta_{KS})S^2 + \delta_{KS}z^2] \} - (-1 + \delta_{KS})S(a_{\text{bh}}^2 \\
& + S^2)\beta) \rho + a_{\text{bh}}^2 (-1 + \delta_{KS})(a_{\text{bh}}^2 S + S^3)^2 z^2 \rho^2] \tilde{S}^2 \\
& - (-1 + \delta_{KS})S^2 (a_{\text{bh}}^2 + S^2)^2 z^2 \rho^2 \tilde{S}^4 \}, \tag{59}
\end{aligned}$$

and $g_{\alpha\beta} = g_{\beta\alpha}$. Also,

$$\delta_{KS} = \frac{2m_{\text{bh}} \tilde{S}^2 S}{\tilde{S}^4 + a_{\text{bh}}^2 z^2}, \tag{60}$$

$$\nu = a_{\text{bh}}^2 + \tilde{S}^2, \tag{61}$$

$$\rho = 2S + \beta, \tag{62}$$

$$\zeta = \frac{\beta^2 (\tilde{S}^2 + a_{\text{bh}}^2 \cos^2(\theta))}{(\beta^2 + 4\tilde{S}^2) \Delta_{KS}}, \tag{63}$$

$$\Phi = \frac{1}{2\Delta_{KS}(S^4 + a^2 z^2) \nu \tilde{S}}. \tag{64}$$

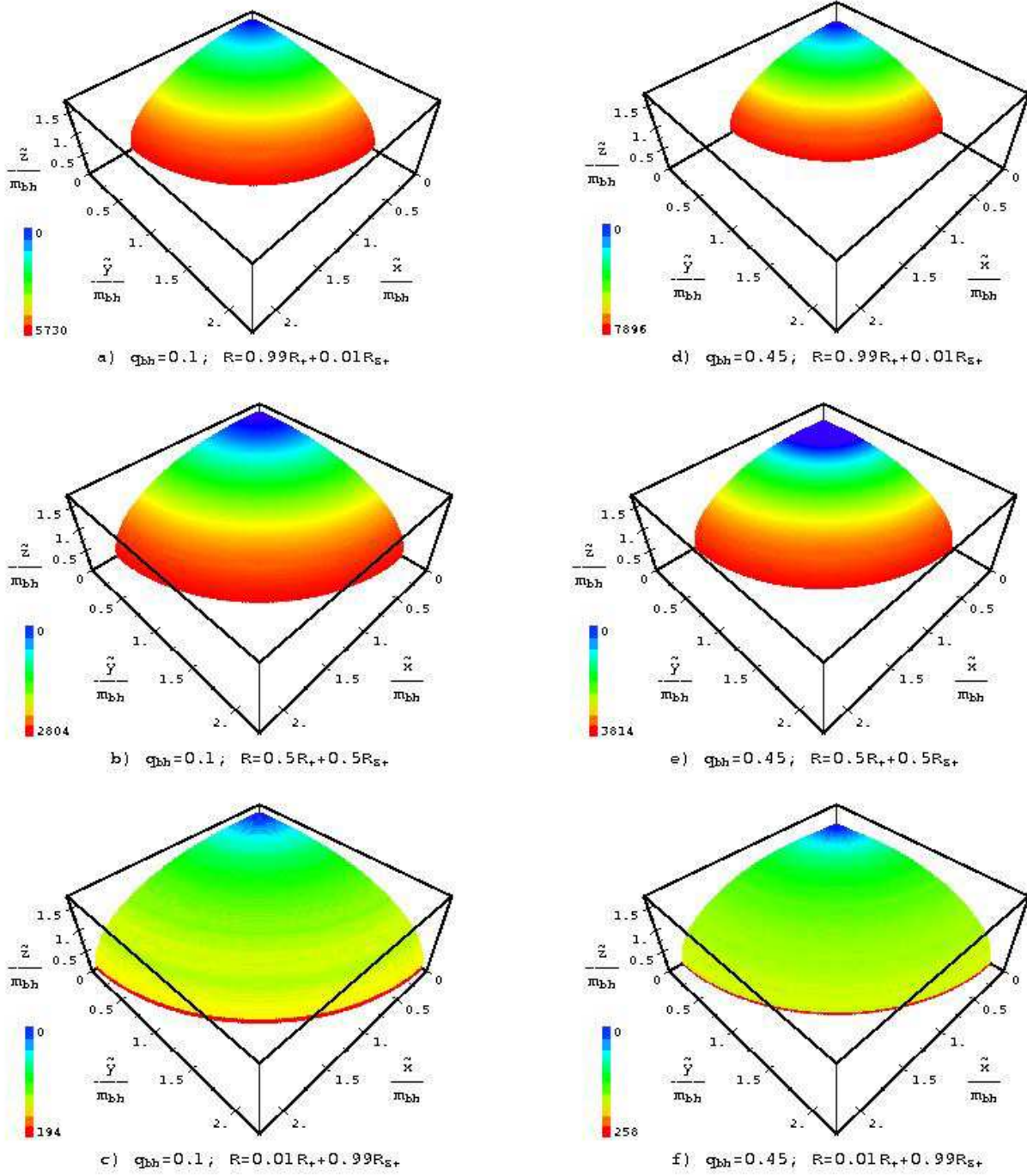
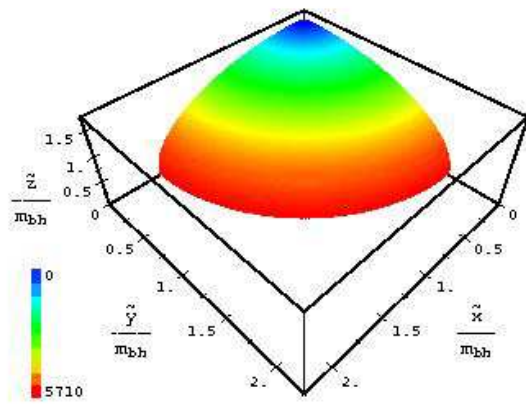
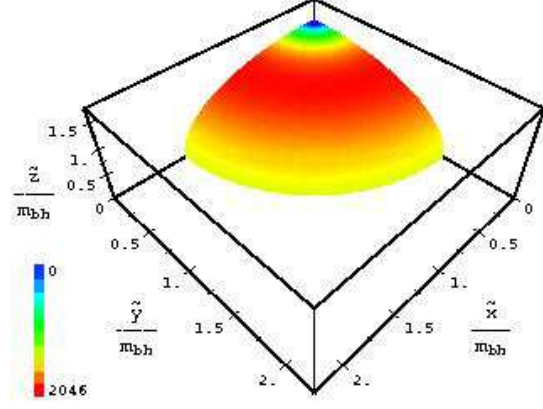


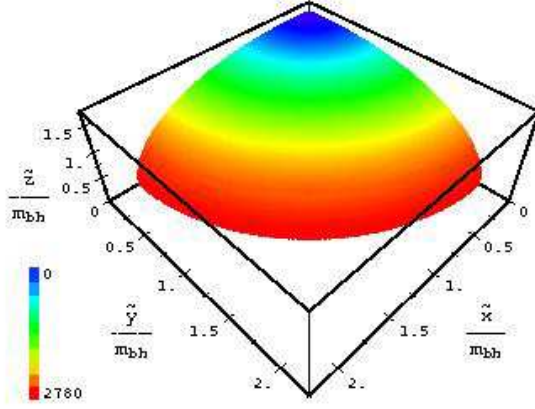
Figure 1: NPV maps for $a_{bh} = m_{bh}\sqrt{3/4}$ for the Kerr-Newman metric. See the text for an explanation of the colour mapping. (a) At the surface $R = 0.99R_+ + 0.01R_{S+}$ with $q_{bh} = 0.1$; (b) at the surface $R = 0.5R_+ + 0.5R_{S+}$ with $q_{bh} = 0.1$; (c) at the surface $R = 0.01R_+ + 0.99R_{S+}$ with $q_{bh} = 0.1$; (d) at the surface $R = 0.99R_+ + 0.01R_{S+}$ with $q_{bh} = 0.45$; (e) at the surface $R = 0.5R_+ + 0.5R_{S+}$ with $q_{bh} = 0.45$; and (f) at the surface $R = 0.01R_+ + 0.99R_{S+}$ with $q_{bh} = 0.45$.



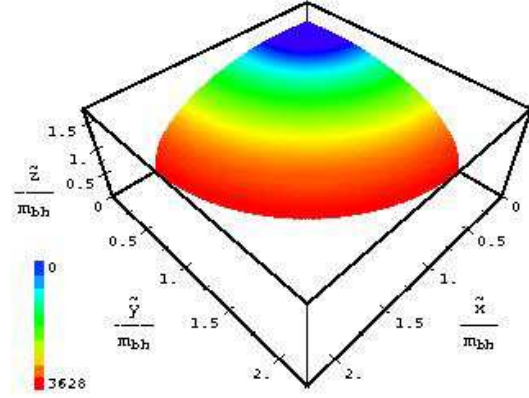
a) $q_{bh}=0.1$; $S=0.99S_++0.01S_{S_+}$



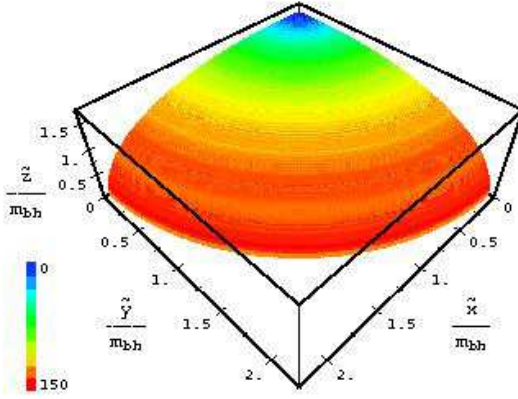
d) $q_{bh}=0.45$; $S=0.99S_++0.01S_{S_+}$



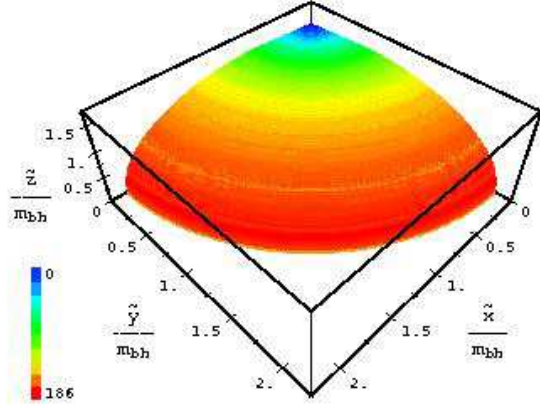
b) $q_{bh}=0.1$; $S=0.5S_++0.5S_{S_+}$



e) $q_{bh}=0.45$; $S=0.5S_++0.5S_{S_+}$



c) $q_{bh}=0.1$; $S=0.01S_++0.99S_{S_+}$



f) $q_{bh}=0.45$; $S=0.01S_++0.99S_{S_+}$

Figure 2: NPV maps for $a_{bh} = m_{bh} \sqrt{3/4}$ for the Kerr–Sen metric. See the text for an explanation of the colour mapping. (a) At the surface $S = 0.99S_+ + 0.01S_{S_+}$ with $q_{bh} = 0.1$; (b) at the surface $S = 0.5S_+ + 0.5S_{S_+}$ with $q_{bh} = 0.1$; (c) at the surface $S = 0.01S_+ + 0.99S_{S_+}$ with $q_{bh} = 0.1$; (d) at the surface $S = 0.99S_+ + 0.01S_{S_+}$ with $q_{bh} = 0.45$; (e) at the surface $S = 0.5S_+ + 0.5S_{S_+}$ with $q_{bh} = 0.45$; and (f) at the surface $S = 0.01S_+ + 0.99S_{S_+}$ with $q_{bh} = 0.45$.